TITLE: Optimization of NSM-CFRP reinforcement on pre-cracked RCB using Taguchi method:

Numerical Analysis

AUTHORS: Fatimaalzhra SHAMMARI,Zeki HASGÜR

PAGES: 93-104

AURUM MÜHENDİSLİK SİSTEMLERİ VE MİMARLIK DERGİSİ
AURUM JOURNAL OF ENGINEERING SYSTEMS AND ARCHITECTURE

Cilt 6, Sayı 1 | Yaz 2022
Volume 6, No 1 | Summer 2022,93-104

ARAŞTIRMA MAKALESİ / RESEARCH ARTICLE

OPTIMIZATION OF NSM-CFRP REINFORCEMENT ON PRE-CRACKED RCB USING TAGUCHI METHOD: NUMERICAL ANALYSIS

Fatimaalzhra Rasim Maseer SHAMMARI[1]
[1]Civil Engineering Department, Altinbas University, Istanbul, Turkey
fatimaalshmary96@gmail.com, ORCID NO: 0000-0001-6103-2282

Zeki HASGÜR[2]
[2]Civil Engineering Department, Altinbas University, Istanbul, Turkey
zeki.hasgur@altinbas.edu.tr, ORCID NO: 0000-0002-7769-5678

GELİŞ TARİHİ/RECEIVED DATE: 29.01.2021 REVİZYON TARİHİ/REVISION DATE:25.03.2022

Abstract
In the current paper, different methods of repairing a pre-cracked reinforced concrete beam (RCB) were reviewed and described briefly. Afterwards, near surface mounted (NSM) technique was used to simulate reinforcement of a pre-cracked RCB using carbon fiber reinforced polymer (CFRP) laminated layer. To do this end, Firstly, based on previous experimental and analytical studies the limitations of the dimensions were specified and then using Minitab software, Taguchi L9 orthogonal array design of experiment (DoE) applied to optimize the number of simulations and find the best dimensions for the reinforcement. Subsequently, ABAQUS software used to analyze the flexural behavior of the NSM-CFRP Pre-cracked RCB. Finally, Force-deflection curves were exported from the simulation results and the best reinforcing pattern was selected.

Keywords: Finite element modeling, Optimization, Reinforced concrete beams, Fiber reinforced polymers, ABAQUS.

TAGUCHI YÖNTEMİ KULLANARAK ÖNCEDEN ÇATLAYAN RCB ÜZERİNDE NSM-CFRP GÜÇLENDİRMESİNİN OPTİMİZASYONU: SAYISAL ANALİZ

Özet
Bu makalede, önceden çatlamış bir betonarme kirişin (RCB) onarımı için farklı yöntemler gözden geçirilmiş ve kısaca açıklanmıştır. Daha sonra, karbon fiber takviyeli polimer (CFRP) lamine katman kullanılarak önceden çatlamış bir RCB'nin takviyesini simüle etmek için yüzeye monte (NSM) tekniği kullanıldı. Bu amaçla, öncelikle önceki deneysel ve analitik çalışmalara dayalı olarak boyutların sınırlamaları belirlenmiş ve ardından Minitab yazılımı kullanılarak, simülasyon sayısını optimize etmek ve en iyi boyutları bulmak için Taguchi L9 ortogonal deney tasarımı (DoE) uygulanmıştır. Daha sonra, ABAQUS yazılımı, NSM-CFRP

Pre-cracked RCB'nin eğilme davranışını analiz etmek için kullanıldı. Son olarak, simülasyon sonuçlarından Kuvvet-sapma eğrileri dışa aktarıldı ve en iyi takviye modeli seçildi.

Anahtar Kelimeler: Sonlu eleman modelleme, Optimizasyon, Betonarme kirişler, Fiber takviyeli polimerler, ABAQUS.

1. INTRODUCTION

Concrete is one of the main materials of all constructions due to the high strength, specifically compressive strength. However, low tensile strength of the concrete is the weakness of this artificial composite. Therefore, strengthening is needed for concrete for the applications which require high tensile strength such as structural parts in constructions and bridges like beams and columns. Commonly, the reinforcement is in the shape of reinforcing bars and welded wire made by steel embedded inside of the concrete.

Steel reinforced concrete beams are the most common version of reinforced beams which have a decent tensile strength as well as appropriate compressive strength. Despite the high tensile strength of the embedded steel inside the concrete beam, still cracking occurs in the bottom part of the beams and with increasing the load they propagate and with progressing the crack propagations the beam failure happens. Furthermore, based on the ACI code, different forms of reinforcements such as structural steel, steel pipe, steel tubing, and high-strength steel tendons can be utilized to reinforce the concrete in terms of increasing tensile strength (CONCRETING, 2017). Several other methods have been also investigated in order to find the most economical reinforcing method of the concrete to reach to the same tensile strength for the reinforced concrete. One of these methods is using short fibers of different materials such as steel, fiberglass, etc.

first the theoretical foundations of deep beams reinforced with FRP are presented and then in order to get acquainted with the studies done on deep beams reinforced with FRP and to find the existing strengths and weaknesses, a number of research done on FRP-reinforced deep beams are provided.

In the case of FRP-reinforced deep beams, there are generally no regulations that specifically address the FRP-reinforced deep beams. For ordinary beams in the existing relations of the regulations, the following expression is used to calculate the shear strength of the reinforced beam:

$$V_n = V_c + V_s + V_{frp} \tag{1}$$

In this regard, is the shear capacity of concrete (including the bearing share of concrete shear, the effect of grain lock and clamp and the lingual effect of beam flexural reinforcements), is the shear strength of Stirrups and is the share of FRP materials in beam shear strength.

(Chaallal et. al., 1998) proposed the following relation for , according to the structure of ACI 318-99:

$$V_{frp} = \emptyset_{frp} A_{frp} f_{frp} \frac{(\sin\beta + \cos\beta)d}{S_{frp}} \tag{2}$$

In this relation, tensile strength of FRP materials and reduction coefficient of resistance for FRP materials, cross section of a pair of FRP strips, β angle of the fibers to the horizon (clockwise), d effective beam depth and distance between FRP strips is along the axis of the beam. In addition, the average shear stress between the FRP material and the concrete intended for the design should not exceed half of the maximum adhesion stress. This model has two main drawbacks. It is assumed that all FRP materials cut by shear cracking have reached their maximum tensile strength, which is conservative in this assumption. Also, this modeling is not consistent with the experimental results in limiting the stress level in FRP materials that are likely to separate.

(Triantafillou et. al., 1998) showed that it is almost impossible to accurately predict the contribution of FRP materials to the shear capacity of the beam. The criteria presented by him are based on European regulations.

$$V_{frp} = \frac{0.9}{\gamma_{frp}} E_{frp} \varepsilon_{frp} \rho_{frp} b_w d(1 + \cos\beta)\sin\beta \tag{3}$$

In the relation above, is the coefficient of elasticity of FRP materials. Also, , where is the thickness of the FRP layer, is the width of the reinforced concrete beam and is the partial safety factor for the tensile strength of FRP materials, the value of which is suggested for CFRP carbon reinforcement composites is 1.15. The main weakness of this modeling is that no special difference is made for different shear .reinforcement designs such as cross-section twisting and gluing to side surfaces as well as failure modes Smith-Teng modeling was performed on the assumption that individual FRP strips could be equated with continuous plates. Therefore, these modeling can be used for both tape and FRP panels. Of course, for FRP tapes, there are some restrictions on the maximum distance between separate tapes. In a general reinforcement design, if the shear cracks are inclined at an inclination θ with respect to the longitudinal axis of the beam, the value of the share of FRP strips in the shear capacity of the beam is equal to:

$$V_{frp} = 2 f_{frp} t_{frp} w_{frp} \frac{h_{frp(\cot\theta + \cot\beta)\sin\beta}}{S_{frp}} \tag{4}$$

In this regard, is the average stress in the FRP strip, below which a shear crack has passed in the final state. is the width of each of these strips, which is measured perpendicular to the position of the fibers in the strip. , the horizontal distance of the strips from each other is β, the angle of inclination of the fibers, which is measured in a clockwise direction relative to the longitudinal axis of the beam on the left side of the fibers.

Although, there are many different methods to reinforced and repair cracked reinforced concrete beams, near surface mounting (NSM) FRP is one of the most common and effective technique which have been used in different studies for different designs and crack patterns (De Lorenzis and Teng, 2007) (Soliman et. al., 2011) (Al-Abdwais et. al., 2016) (El-Gamal et. al., 2016). In line with these studies, there is a lack of numerical study to investigate the effect of dimensions (length, width, and thickness) of CFRP layer on the flexural behavior of pre-cracked RCB. In this paper, the aforementioned effect was investigated after implementing Taguchi method as a design of experiment (DoE) technique to optimize the number of simulations and find the most optimum parameters.

2. NUMERICAL MODELLING

ABAQUS V6.21 was utilized to simulate all the conditions and numerically analyze them. ABAQUS is a famous finite element software which is very user friendly, and it can be employed for analyzing an extensive linear and non-linear model. Various mechanical properties such as elastic modulus, stress-strain, density, damage criteria include Hashin and inelastic damages for steel, concrete and FRP materials were defined in property section of ABAQUS. It is worth noting that the damage criteria for all materials were performed using concrete damage plasticity (CDP) model. For all loading sections include elastic region and plastic region isotropic damaged plasticity theory is used (ABAQUS and Manual, 2012). The CDP model and related parameters are shown in Table 1.

The experimental results from the literature were used to identify both compressive and tensile stress vs strain chart of the concrete for the simulation. The relevant formula for compression and tension are listed below, respectively. It must be noted that these relationships are credential for the uniaxial loading.

$$\sigma_c = E_0 \, (1 - d_c)\left(\varepsilon_c - \varepsilon_c^{pl}\right) \tag{5}$$

$$\sigma_t = E_0 \, (1 - d_t)\left(\varepsilon_t - \varepsilon_t^{pl}\right) \tag{6}$$

Where in these formulas , , , are the compressive stress, compressive damage variable and the elastic modulus of the concrete, separately. Furthermore, for the second equation, , , , are tensile stress, tensile damage variable, correspondingly. Moreover, is compressive strain and is compressive plastic strain, respectively. Lastly, and are the strain under the tension and tensile plastic strain, respectively.

Table 1. CDP parameters of Concrete (Lee and Fenves, 1998).

Dilation Angle (Ψ)	Eccentricity (Є)	fb_0/fc_0	K	Viscosity (μ)
56	0.1	1.16	0.667	0.0001

On the other hand, another model progressed by (Bahij et. al., 2018) was performed in ABAQUS to simulate the failure of the concrete. The aforementioned model has been modified by different investigators (Lee and Fenves, 1998). The mechanical properties in plastic regions must be explained using the different phenomena such as deterioration of material strain softening and hardening as well as volumetric expansion which subsequently decreases stiffness and strength of concrete. furthermore the extensive information and other theories related to CDP model can be found in ABAQUS Analysis User's Manual (Manual, 2012).

Furthermore, the plastic behavior for strain and stress throughout the damage of concrete can be attained by the Equations (7) and (8). Also, the degradation can be happened in the softening section where stiffness is relational to the cohesion of the beam.

$$\frac{E}{E_0} = \frac{C}{C_{max}} = (1-d) \tag{7}$$

$$\varepsilon^{-p} = \varepsilon^{p} - \frac{d}{1-d}\frac{\sigma}{E_0}$$
$$\varepsilon^{-p} = \varepsilon - \frac{f}{E_0} \tag{8}$$

In above equations C is cohesion, which is also proportional to stress, C_{max} represents the concrete's strength, and also, d and f are damage parameter and the compressive or tensile strength of concrete. Moreover, damage compression for model elements and tensile parameters are determined by Equations (9) and (10), independently.

$$d_c = 1 - \frac{\sigma_C E_C^{-1}}{\varepsilon_c^{pl}\left(\frac{1}{bc}-1\right) + \sigma_c E_C^{-1}} \tag{9}$$

Which σ_c is the stress in the compression mode, and σ_t is stress in the tension mode. E_c is the concrete modulus elasticity, is the plastic part of the strain. The parameters include of b_c and b_t are suggested by (Barbato, 2009) and which are set as 0.7 and 0.1, respectively.

The cracks under the reinforced concrete beams which happening when the beam is under the flexural loading and bending, are the most common types of cracks. These cracks initiate in the bottom part of the beam and propagate through the central regions and subsequently cause the failure of the beam. The reason that these cracks starts from the bottom of the beam is low tensile strength of the concrete and the tension appears at the bottom part of the beam when it is under the flexural loading. Therefore, flexural loading was used in the current thesis to observe the behavior of reinforced beam after initiation of the cracks.

In this thesis four-point bending experiments were numerically analyzed and simulated in ABAQUS, where the schematic of the reinforced concrete beam with embedded steel bars and stirrups are shown in Figure 3.1. Th dimensions of the beam have been shown in the figure where width, height and length were chosen based on the consistency with the other experimental and numerical works as 300 mm, 200mm, and 2400 mm, respectively.

Furthermore, as it is mentioned in the schematic, the beam has been reinforced using four long bars which the diameters of them are 8 mm and series of stirrups via an interval spacing of 0.1 m c/c (Shown in Figure 3.1). The elastic modulus of the commercial steel for different parts of the reinforcements such as bars and stirrups has been chosen and stated as 200 GPa. Moreover, other mechanical properties of the elements were defined and written in ABAQUS to provide the necessary information for the analysis. Also, compressive strength (fc) of the concrete employed in this thesis was 30 MPa.

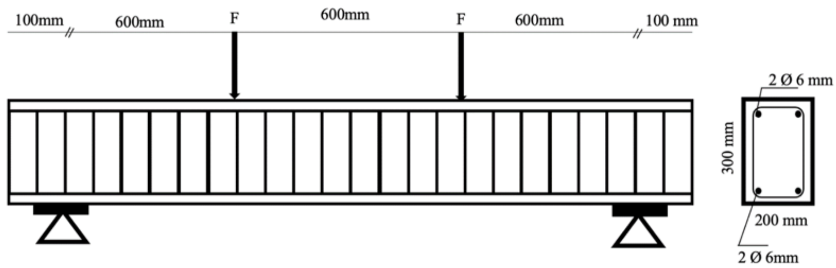

Figure 1. Schematic of reinforced concrete beam under the four-point bending experiment with the dimensions of the bars and stirrups inside the beam.

Based on the experimental results mechanical properties of the concrete which has used in the simulation is listed below in Table 2. Two different criteria have been considered to achieve the best results in numerical modeling. The first one was concrete damage plasticity (CDP) which is important when we want to investigate the damage behavior of structure after yield point to see the behavior of the plastic region and crack initiation and propagation. Also, the other important criteria are dynamic mechanical behavior of the concrete which is very crucial to predict the behavior of the concrete based structured after applying flexural load on them. The Dynamic behavior of concrete utilized for the numerical analysis as well as damage behavior employed in ABAQUS is shown in Table 2.

Table 2. Dynamic mechanical properties and tensile damage behavior of concrete.

Tensile (CDP)			Tensile Damage	
Stress(Pa)	in-strain(Pa)	stress(Pa)	damage(Pa)	in-strain(Pa)
3450652.112	0	3450652	0	0
2295713.038	0.00029	2295713	0.740058	0.00029
1884035.156	0.000549	1884035	0.868129	0.000549
1651583.006	0.000802	1651583	0.916419	0.000802
1496056.714	0.001052	1496057	0.940729	0.001052
1382096.603	0.0013	1382097	0.955019	0.0013

Totally, nine reinforced concrete (RC) beams were modeled and simulated in this paper. The beams have the dimensions of 300mm x 200mm x 2000mm with an embedded region consists of a series of stirrups and four bars at the corners of the stirrups. The yield and elastic modulus of steel used in the simulations were defined ad 450 MPa and 200 MPa, respectively. Furthermore, the interactions between all the parts of the setup were defined and friction properties also was added between the concrete and CFRP reinforcement material. Also, between supports and beam the encastre boundary conditions were defined, so the beam can just deform and slip on the support, therefore, support will be fixed (see Figure 2).

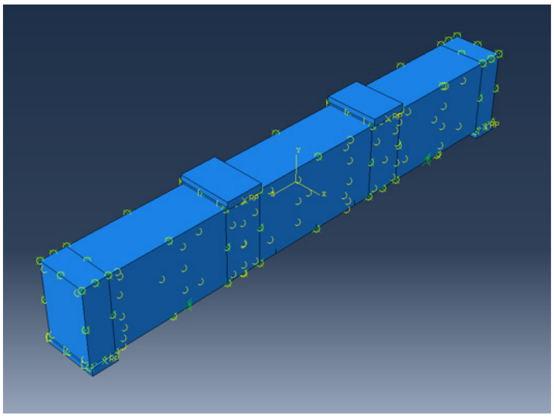

Figure 2. The interactions defined to the system between all the parts.

The design of the setup after meshing is shown in Fig 3. Afterward, in mesh module all the parts were meshed one by one to discretize the parts for numerical solution. Although, low element size may give better results, the low element size increases the number of the elements which subsequently increase the simulation time. Therefore, we have tried to optimize the number of the elements and element size to achieve a reliable result and compute the problem faster. In most of the cases of this thesis, the approximate global size was defined as 0.05. Figure 3. demonstrates the system for the four-point bending test after mesh.

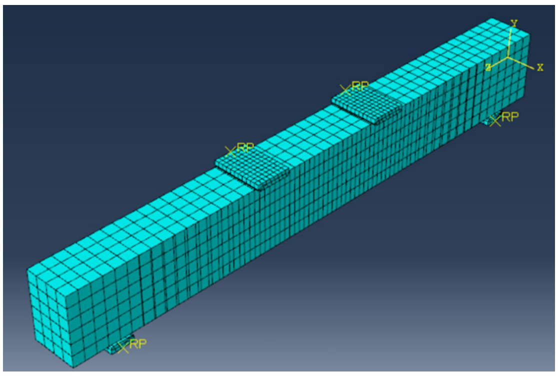

Figure 3. Design of setup after mesh.

3. RESULTS AND DISCUSSION

CFRP laminated reinforcements were used in the simulation in order to repair and decrease the crack initiation and subsequently crack propagation in the tension part of the concrete beams. In order to find the most optimum parameters for the FRP reinforcement, different optimization systems were employed. To do this, Taguchi's optimization method was used to optimize the dimension of the FRP reinforcement covered bottom part of the beam. L9 orthogonal array was chosen from the various types of Taguchi method in order to minimize the number of simulations. The parameters with the levels for each of them have been listed in Table 3. Three parameters of width, length, and thickness of FRP were used as the variables, and three levels for each of these parameters were selected to fill the simulation sets.

Table 3. Dimensions of the FRP layer to repair the bottom part of the RCB.

Parameter	Level 1 (mm)	Level 2 (mm)	Level 3 (mm)
Length	1400	1800	2000
Width	100	150	200
Thickness	0.5	1	2

After applying L9 orthogonal array Taguchi method, the experimental set of parameters were selected as shown in Table 4. Minitab V20.4 was used to create the Taguchi analysis design with aforementioned parameters and level sets. Also, the maximum load at failure was selected as the response factor of the simulation sets.

Table 4. Simulation set numbers with respective parameters.

Simulation Set Number	Length (mm)	Width (mm)	Thickness (mm)
1	1400	100	0.5
2	1400	150	1.0
3	1400	200	2.0
4	1800	100	1.0
5	1800	150	2.0
6	1800	200	0.5
7	2000	100	2.0
8	2000	150	0.5
9	2000	200	1.0

All the conditions were simulated using the same initial crack patterns and the load at failure of the beam was exported from the ABAQUS software results, and subsequently the load vs deflection curves were formed in Origin Pro 2021b software. The results of the simulations for each condition were extracted from ABAQUS and can be seen in Figure 4.

It can be seen the highest force at the failure value is related to the set 5 parameters with length, width, and thickness of 1800, 150, and 2 mm, respectively. This can be attributed to the effect of covering all the length of the beam at the bottom surface of the beam as well as the high effect of 2 mm thickness on the increasing the strength of the pre-cracked RCB against the tension applied on the downside of the beam in flexural loading. Also, it can be asserted that increasing the width of the CFRP layer is not necessary after 150mm due to the blocking effect of the layer on the cracks throughout the length of the beam which can cover all the cracks. Also, based on the results of the flexural loading simulation, it can be concluded that covering all the beam length through the supports at both sides are not necessary and even can decrease the effect of the CFRP layer. This can be due to the softening effect of the polymer layer in the interaction points between the supports and beam where this layer can be torn in the edge of the supports.

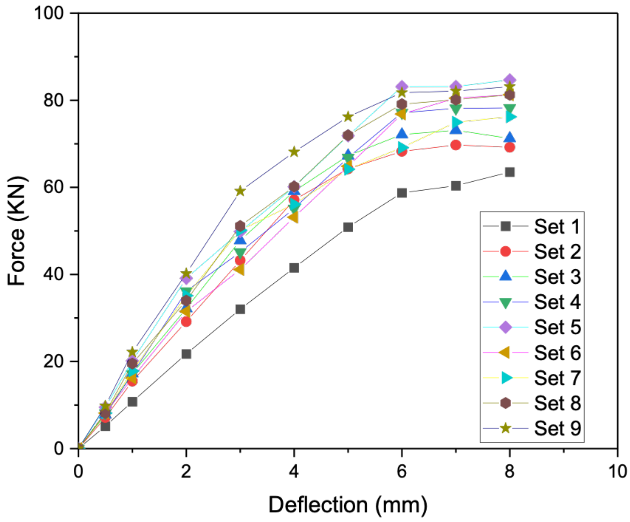

Figure 4. Force vs Deflection curves of different simulation sets.

The response factor was set as force at the failure in L9 orthogonal array Taguchi method and based on the results of the simulations, the response table for means was exported and shown in Table 4.3. Furthermore, the main effect plot for means was extracted from Minitab and demonstrated in Figure 5. As it shown in the curves, it can be seen that the effect of increasing length of the CFRP layer from 1400mm to 1800mm was very critical to increase the force at the failure value. However, after reaching to the support part there is no need to increase the length up to the end of the beam.

Moreover, the effect of increasing the width and thickness of the layer became steady after reaching to the middle level of 150 and 2 mm, respectively. This can be attributed to the covering the main cracks along the beam with 150mm width. Also, the outside layer of the CFRP cannot affect too much on propagation of the pre-defined cracks, therefore, increasing the thickness from 1 to 2 mm is not necessary.

Level	Length	Width	Thickness
1	67.99	72.65	75.35
2	81.38	78.38	76.86
3	80.20	78.55	77.36
Delta	13.39	5.90	2.02
Rank	1	2	3

Table 5. Response table for means extracted from Minitab software for L9 orthogonal array Taguchi method.

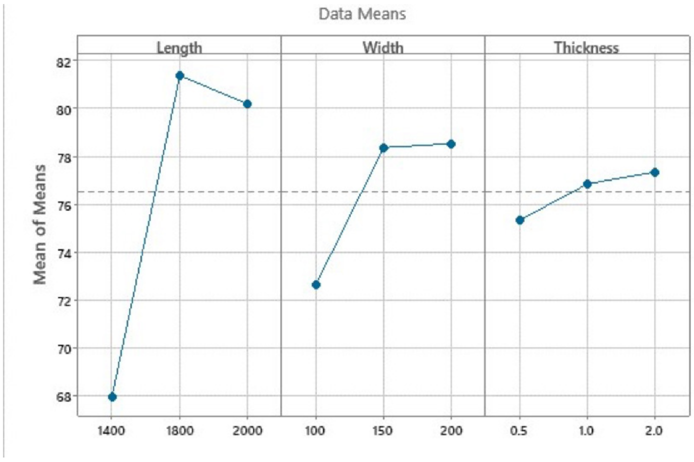

Figure 5. Main effects plot for means in L9 orthogonal array Taguchi method exported from Minitab software.

4. CONCLUSIONS

In this paper the effect of CFRP dimensions on the flexural behavior of the reinforced concrete beam were investigated using numerical analysis. To this end, L9 orthogonal array Taguchi method was used to set the parameters of each condition. Minitab V20.4 was used to create the Taguchi analysis design with aforementioned parameters and level sets. The response factor was chosen as force to failure after 8 mm deflection and the main conclusions were as follows:

i. The highest force at the failure value is related to the set 5 parameters with length, width, and thickness of 1800, 150, and 2 mm, respectively which can be due to the effect of covering all the length of the beam at the bottom surface of the beam as well as the high effect of 2 mm thickness on the increasing the strength of the pre-cracked RCB against the tension applied on the downside of the beam in flexural loading.

ii. Also, it can be asserted that increasing the width of the CFRP layer is not necessary after 150mm due to the blocking effect of the layer on the cracks throughout the length of the beam which can cover all the cracks.

iii. Furthermore, based on the results of the flexural loading simulation, it can be concluded that covering all the beam length through the supports at both sides are not necessary and even can decrease the effect of the CFRP layer.

iv. Moreover, the effect of increasing the width and thickness of the layer became steady after reaching to the middle level of 150 and 2 mm, respectively. This can be attributed to the covering the main cracks along the beam with 150mm width.

5. REFERENCES

ABAQUS, U. s. M. and C. U. s. Manual. 2012. Dassault Systemes Simulia Corp, Providence, RI, USA, 6(1).
Al-Abdwais, A., and R.J.C. Al-Mahaidi. 2016. Modified cement-based adhesive for near-surface mounted CFRP strengthening system, 124: 794-800.

Bahij, S., S.K. Adekunle, M. Al-Osta, S. Ahmad, S.U. Al-Dulaijan and M.K. Rahman. 2018. Numerical investigation of the shear behavior of reinforced ultra-high-performance concrete beams, Structural Concrete, 19(1): 305-317.

Barbato, M. 2009. Efficient finite element modelling of reinforced concrete beams retrofitted with fibre reinforced polymers, Computers & Structures, 87(3-4): 167-176.

Chaallal, O., M.-J. Nollet, and D. Perraton. 1998. Strengthening of reinforced concrete beams with externally bonded fiber-reinforced-plastic plates: design guidelines for shear and flexure, 25(4): 692-704.
CONCRETING, C. W. J. A. C. 2017. ACI 306R-16.

De Lorenzis, L. and J.G. Teng. 2007. Near-surface mounted FRP reinforcement: An emerging technique for strengthening structures, 38(2): 119-143.

El-Gamal, S., A. Al-Nuaimi, A. Al-Saidy, A.J.C. Al-Lawati. 2016. Efficiency of near surface mounted technique using fiber reinforced polymers for the flexural strengthening of RC beams, 118: 52-62.

Lee, J. and G.L. Fenves. 1998. Plastic-Damage Model for Cyclic Loading of Concrete Structures, Journal of Engineering Mechanics, 124(8): 892-900.

Manual, A.S.U.s. 2012. Abaqus 6.11, http://130.149, 89(2080): v6.

Soliman, S.M., E. El-Salakawy and B. Benmokrane. 2011. Bond performance of near-surface-mounted FRP bars, 15(1): 103-111.

Triantafillou, T. 1998. Shear strengthening of reinforced concrete beams using epoxy-bonded FRP composites, 95: 107-115.